Outstanding durability of sol-gel thermal barrier coatings reinforced by YSZ-fibers

E. Delon[a,*], F. Ansart[a], S. Duluard[a], J.P. Bonino[a], D. Monceau[b], A. Rouaix[b], R. Mainguy[b], C. Thouron[b], A. Malié[c], A. Joulia[d], L. Bianchi[c], P. Gomez[e]

[a] CIRIMAT, Université de Toulouse, CNRS, INPT, UPS, Université Toulouse 3 Paul Sabatier, Bât CIRIMAT, 118 Route de Narbonne, 31062 Toulouse cedex 9, France
[b] CIRIMAT, Université de Toulouse, CNRS, INPT, UPS, CIRIMAT-ENSIACET INP-ENSIACET, 4 allée Emile Monso, BP 44362, 31030 Toulouse cedex 4, France
[c] SAFRAN AIRCRAFT ENGINES Site de Chatellerault, ZI Nord, rue Maryse Bastié, BP 129, 86101 Chatellerault Cedex, France
[d] SAFRAN Tech, Pôle Matériaux et Procédés, rue des Jeunes Bois, Châteaufort, CS 80112, 78772 Magny-Les-Hameaux, France
[e] DGA Techniques aéronautiques, 47 rue Saint Jean - 93123, 31131 Balma, France

ARTICLE INFO

ABSTRACT

Thermal barrier coatings (TBC) were fabricated with commercial powders of yttria stabilized zirconia with spherical and fiber-like morphologies. The influence of fiber percentage and sintering temperature on the thermomechanical behavior was studied. TBCs with 60%-80% fibers content had the best lifetime in cyclic oxidation with less than 10% of coating spallation after 1000 cycles, with very good reproducibility. They reached lifetimes higher than industrial TBCs made by EB-PVD. The enhancement of durability is believed to be due to an increase in the thermomechanical constraints accommodation thanks to higher porosity and higher tenacity due to the presence of well anchored fibers, indeed deviation of the cracks were observed. Moreover, the morphology of the thermally grown oxide (TGO) layer is also favorable as it includes anchorage points of the TGO with fibers. This increased the adherence at the substrate interface and improved lifetime.

1. Introduction

Thermal barrier coatings systems (TBC) protect critical metallic parts of aircraft engines such as gas turbine blades and combustion chambers. They improve gas turbines efficiency and durability because of their excellent thermal insulation properties [1,2]. TBC are usually deposited by air plasma spraying (APS) or by Electron beam vapor phase deposition (EB PVD). Sol gel is an innovative process to deposit such coatings on engine parts, with many potential advantages on the other processes. The sol gel method is a versatile process resulting from the wet route which allows working at room temperature during coating deposition.

A typical TBC consists of: *(i)* a top coat layer: the TBC itself, a thermal insulating porous ceramic coating, generally made of yttria partially stabilized zirconia (YSZ), *(ii)* an intermediate thermally grown oxide (TGO) layer along the metal ceramic interface. TGO is formed during exposure at high temperatures from the metallic bond coat, it consists predominantly of alumina. *(iii)* An aluminium rich bond coat which improves the cohesion between the metallic substrate and the TBC, and *(iv)* the nickel based superalloy that supports mechanical loading.

Each layer has its own behavior and its thermal and mechanical properties leading to thermomechanical stresses. Indeed, upon processing and "in service" high temperature exposure, there are establishment of internal stresses. Furthermore, the TGO continuously grows at the bond coat/TBC interface. The increase in the TGO thickness induces local stresses that lead to the failure of TBC. Indeed the usual mechanism of TBC failure is linked to the spallation at or close to the TGO interfaces. The delamination takes place either in the ceramic YSZ layer or the metallic bond coats for the EB PVD TBCs [3 5], or in the top coat in the vicinity of the TGO for APS top coats on rough bond coatings [6,7].

There are many processes to deposit ceramics TBCs. Industrially, on the turbine blade, the ceramic coating is often deposited by electron beam physical vapor deposition (EB PVD). In the combustion chamber, aircraft manufacturers use the air plasma spray process (APS). Moreover, other processes are under study and evaluation to fabricate TBCs. Among them, one can cite: the suspension plasma spraying (SPS) [8], spark plasma sintering (SPS) [9], metalorganic chemical vapor deposition (MOCVD) [10], sol gel route [11] or electrophoretic deposition [12]. To optimize the TBC mechanical properties and therefore to obtain a good durability of this system, it is necessary to adapt the

* Corresponding author.
E-mail address: elodie.delon@gmail.com (E. Delon).

coating porosity. One solution is to play on the process to change the morphology of the microstructure. For example with EB PVD, TBCs exhibit a porous columnar microstructure resulting in a quite high strain tolerance but a moderately high thermal conductivity. On the other side, APS TBCs have a lamellar dense microstructure resulting in a lower thermal conductivity but a weaker strain tolerance. Another solution is to add pore forming agent, like PMMA, during processing to improve the durability and the efficiency of TBCs[13,14]. By modifying the porosity, thermomechanical properties are improved and the thermal conductivity is reduced [15 17].

Porosity, and therefore thermomechanical properties of sol gel TBCs, can be optimized by working on the morphology of YSZ powders. Indeed, many studies were performed on sol gel TBCs at the Cirimat laboratory. In previous studies, the sol gel TBCs were prepared with YSZ aerogel powders and durability above 1000 cycles of 1 h at 1100 °C could be observed [11,18,19].

In the present work, we work in partnership with the motorist Safran and the French Defense Procurement Agency (DGA). To respect the industrial specifications and to ensure a sustainable supply, commercial powders were used. This change impacted the protocol for the fabrication of sol gel TBCs as the morphology of aerogel powder is very different from commercial powders. To make sol gel TBCs, two types of commercial YSZ powders were used: particles with a spherical morphology (6 mol% Y_2O_3) and fibers (4 mol% Y_2O_3). Indeed, fibers can reinforce porous ceramics and improve mechanical properties of materials [20 24].

Due to the volume expansion (about 4.5%) during the zirconia martensitic transition, which results in irreversible damages, YSZ powders are made of the "non transformable" metastable tetragonal YSZ phase, called t'. This phase does not suffer from the transformation to the monoclinic phase under stresses [25 27]. However, there are not enough studies about porous ceramics to determine which phase between metastable tetragonal t' phase, metastable tetragonal t" phase and cubic c phase has the best mechanical properties at high temperatures. Therefore, sol gel TBCs are manufactured from metastable tetragonal phase t', like typical YSZ TBCs which are generally composed of around 9 mol% of yttria.

The aim of this paper is to define the optimized sol gel TBCs route, in order to optimize the lifetime under cyclic oxidation. The objective is to equal or improve the thermal cycling resistance as compared to a typical TBCs made by EB PVD. To do so, the influence of different parameters such as the percentage of fibers in the powder matrix and the temperature of thermal treatment of TBCs were investigated. Finally, to evaluate the lifetime of sol gel TBCs, TBCs were tested under cyclic oxidation using a standard cycle. In parallel, the porosity of these systems were characterized in order to correlate this parameter with the thermal cycling life.

2. Material and methods

2.1. Substrate pre treatment

Metallic substrates (discs with a diameter of 25 mm) were β (Ni, Pt) Al coated first generation superalloys AM1 provided by Safran Group. AM1 samples were cut from bars by wire electro erosion machine (electro filter). The front face was rectified and the edges were radiated, while the rear face is rough and has sharp edges. Moreover, the bond coating fabrication was optimized for the front face. These differences between the two faces play a crucial role in lifetime of TBCs. Indeed, the barriers on the rear face had a reduced lifetime compared with that of the front face.

The bond coating is a single phase β (Ni, Pt) Al and it is fabricated by platinum deposition via an electrolytic process, followed by diffusion heat treatment under vacuum and a vapor phase aluminization (APVS).

Finally, the β (Ni, Pt)Al coated AM1 samples were grit blasted with corundum before being oxidized in a preheated furnace in air at 1100 °C for 1 h and the cooling was made according to the inertia of the box furnace. The obtained TGO thickness is approximately equal to 1 μm. According to fluorescence spectroscopy Raman analyses, the TGO is only composed of the stable alpha alumina phase. This last point is important because the sol gel TBCs will not be impacted by allotropic transformation of alumina that would alter their lifetime during cyclic oxidation.

2.2. Fabrication of sol gel TBCs

An yttria stabilized zirconia YSZ sol was made from zirconium (IV) propoxide (Sigma Aldrich) and yttrium (III) nitrate hexahydrate (Sigma Aldrich). In order to avoid excessive thermomechanical stresses and thus to obtain the tetragonal metastable t' phase, yttrium nitrate hexahydrate is added in the desired molar proportions: 9.7 mol% $YO_{1.5}$; thus allowing the stabilization of the tetragonal metastable phase. The concentration of zirconium propoxide is set at 0.5 mol/L. The ratios of hydrolysis rate ($[H_2O]/[precursors]$) and the complexation rate ($[Acetylacetone]/[precursors]$) are respectively equal to 8.7 and 0.7.

In parallel, a suspension was realized from YSZ particles; with tetragonal metastable t' phase. A powder with a spherical morphology from TOSOH, with 10 mol% of $YO_{1.5}$ and an average grain size inferior to 1 μm was used for the YSZ particles (Fig. 1a) ; while fibers provided by Zircar Zirconia contained 6 mol% of $YO_{1.5}$, have an average diameter between 5 and 10 μm and an average length in the range of 10 and 50 μm (Fig. 1b). Such fibers have an internal and open porosity (Fig. 1c).

Then, the YSZ sol was added to the suspension to form slurry. The protocol is described on the Fig. 2. The percentage of YSZ fibers (%F) is based on the total mass of YSZ fibers and powders.

YSZ based slurries were deposited by dip coating technique with a Nima Technology Micro Processor Interface IU4 device dip coater, onto

a) Particles with a spherical morphology

10 nm

b) Fibers

10 μm

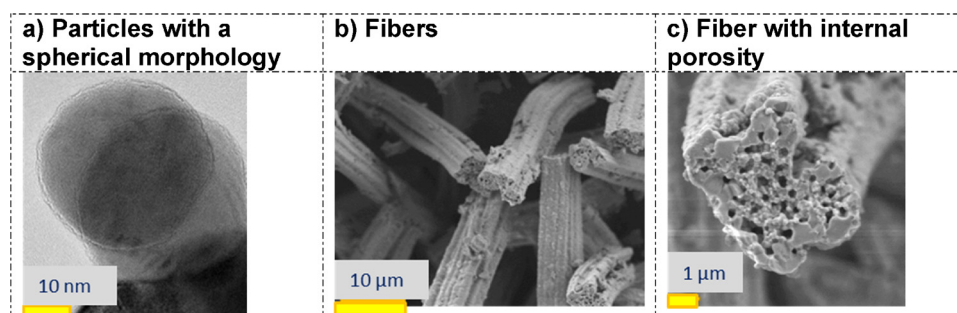**c) Fiber with internal porosity**

1 μm

Fig. 1. Commercial powders of YSZ used to elaborate sol-gel TBC: (a) particles with a spherical morphology (TEM micrographs); (b) fibers (SEM-FEG micrographs); (c) fiber with internal porosity (SEM-FEG micrographs).
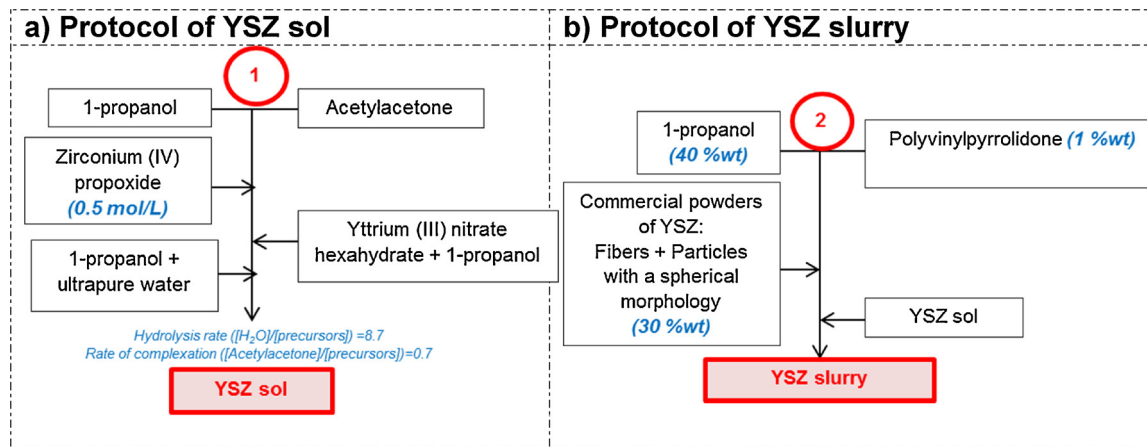
Fig. 2. Protocols used to make: (a) sol of YSZ sol and (b) YSZ slurry.

metal substrates. The depositions were carried out by controlling the withdrawal dip coating velocity (at 400 mm/min) in a chamber with both controlled temperature (between 20 and 25 °C) and relative humidity between 60% and 80%. Many immersions were performed in order to reach the suitable layer thickness which is about 150 200 μm. First, in order to favor the anchorage of the TBCs, a pre bonding layer was deposited onto substrate from the YSZ sol.

Finally, after complete deposition, a first heat pre treatment in air at 600 °C for 1 h was performed to remove organic materials due to the YSZ sol residues. Then, a second heat treatment at 1100 °C or at 1250 °C for 2 h in air (up/down ramp: 50 °C/h) was carried out on the TBC to sinter it and to obtain a good stress resistance. It has been demonstrated by Safran that the substrate does not undergo thermal degradation during the thermal treatment at 1250 °C.

Two main parameters were tested in this study: the percentage of fibers in TBCs and the temperature of the second heat treatment. Percentage of fibers ranging between 0 %F and 80 %F were used to determine for which fiber content the lifetime of the sol gel TBCs was optimized. Heat treatment temperatures of 1100 °C and 1250 °C were chosen as particle sintering starts at 1100 °C. Furthermore, the cyclic oxidation is made at 1100 °C, so if the particles are sintered at 1250 °C, the cohesion between fibers and the powder matrix may be improved. Of course, a heat treatment at 1250 °C may modify the gamma/gamma prime γ γ' superalloy microstructure, and may cause a significant growth of the TGO prior to thermal cycling, and this needs to be kept in mind when analyzing the results.

2.3. Cyclic oxidation

Before cyclic oxidation, the TBCs are cleaned in an ethanol bath and dried with hot, dry and dust free air to remove any impurities that may cause premature spalling. TBCs were characterized by cyclic oxidation in air in an open furnace working at 1100 °C. A cycle is composed of 1 h dwell at 1100 °C (including a very rapid heating) and a cooling of 15 min to room temperature (using a high flow of air, free from oil and pollution). In the furnace TBCs were positioned vertically on sample holders and it is this assembly that moved according to the cycle. The resulting thermal cycling is consistent with the one performed by the motorist Safran. About every 50 cycles, TBCs were weighted with a SARTORIUS GENIUS ME 215 P precision balance and were photo graphed to determine mass variation and the percentage of surface spalling respectively. For comparison, a TBC system with a top coat made by EB PVD and provided by Safran Aircraft Engines was added to the test to serve as a reference. Compared to a sol gel TBC system, the TBC system manufacturing using EB PVD has only one face and a thickness of TGO around 200 nm. Concerning the mass variation, it takes into account both faces of the sol gel TBC samples, namely the
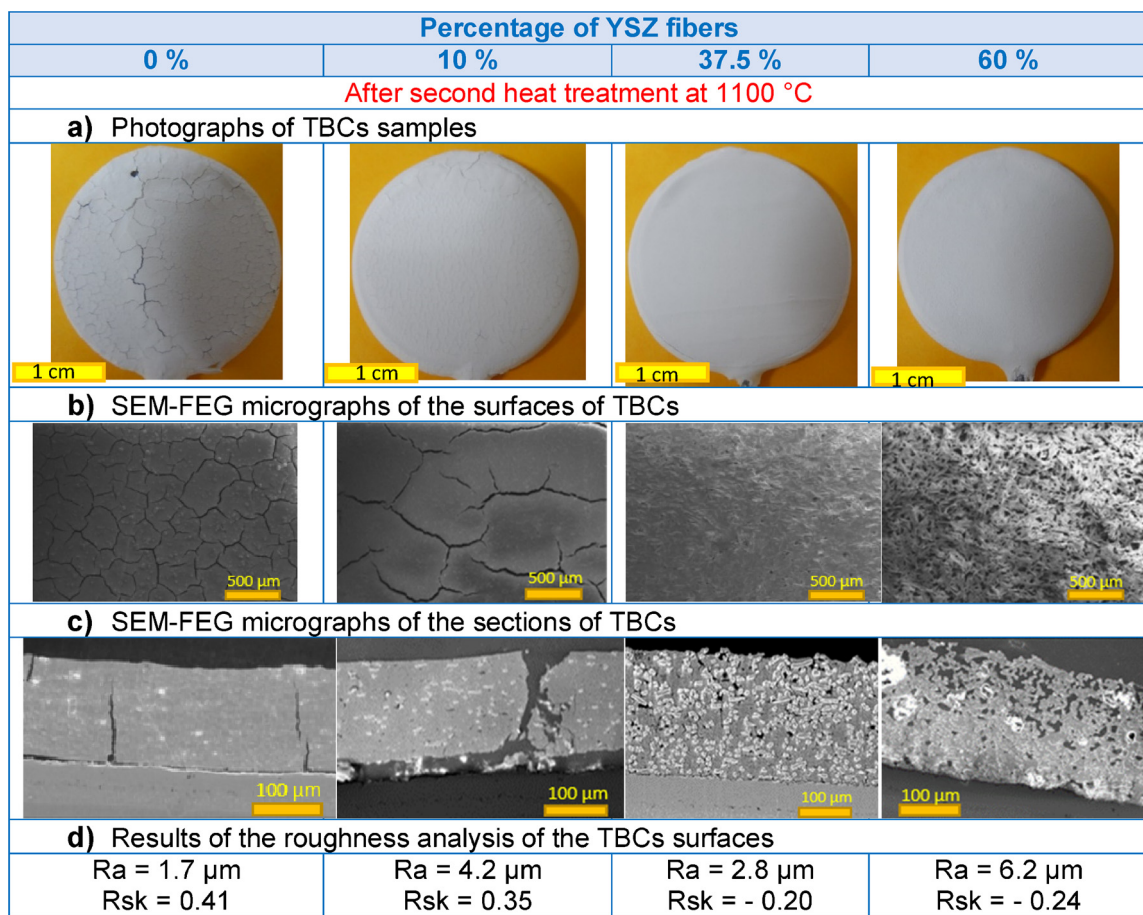
front face rectified and the rear face that is rough. On the other hand, the percentage of surface spalling identified by photography concerns only the front face (rectified). According to Safran standards, a TBC must have a lifetime equal to or greater than 500 cycles with a per centage of mass loss lower than 25 %m and a percentage of surface spalling less than 20 %S. Image analyses were performed with the ImageJ software (GitHub) to determine the percentage of surface spalling. The thicker edge parts are excluded from the analysis since not representative of the normal behavior of the systems.

In order to identify the system with the optimum composition, the mass loss was compared to the surface spalling. Both spalling mea surements must be analyzed in order to conclude on a system. When the mass of the sample is measured, the obtained value takes into account the delamination of the thermal barrier, but also the mass gain due to oxidation. The mass change due to the formation and spalling of the oxide scale on the metallic substrate could cause variations in the ob tained mass values up to nearly 10% of the total mass variation. Furthermore, both faces of the substrate have not been treated in the same way, thus causing preferential delamination of the thermal barrier on the rear face of the substrate rather than that located on the front face. Moreover, a small part of the substrate, a metallic rod used to hold the sample, although cut at the edge of the substrate before cyclic oxidation, is responsible of a loss of mass that can reach 30% of the total mass variation. Thus, it is not uncommon for the percentage of mass loss to fall sharply as the ceramic coating on the rear face has under gone a complete delamination causing a sudden decrease in the value of the total mass. Moreover, it is not uncommon to obtain a coating with a greater thickness at the edges of the substrate. Because of this accu mulation of material, the thermal barrier is preferentially delaminated at the edges. It is therefore very difficult to conclude on the analysis of mass loss alone. As for mass loss, the analysis of the percentage of surface spalling cannot conclude with certainty the suitability of a system. Indeed, this analysis is done from photographs taken at regular intervals of the samples. This method is less sensitive than a weighing (sensitivity about 10 μg for the mass versus 0.1 mm² for the surface). It is therefore interesting to combine the two analyzes in order to con clude on a system.

2.4. Characterization techniques

Before all characterizations (Raman, SEM FEG …), the TBCs sam ples are cleaned in an ethanol bath and dried with hot, dry and dust free air to remove any contamination that may lead to an incorrect analysis.

TBC systems were characterized by fluorescence spectroscopy using a Raman Horiba Jobin Yvon Labram HR 800 spectrometer equipped with a confocal microscope and a 532 nm laser; to check the transfor mation or not of phases of ceramic phases.

Percentage of YSZ fibers			
0 %	10 %	37.5 %	60 %
After second heat treatment at 1100 °C			
a) Photographs of TBCs samples			
1 cm	1 cm	1 cm	1 cm
b) SEM-FEG micrographs of the surfaces of TBCs			
500 µm	500 µm	500 µm	500 µm
c) SEM-FEG micrographs of the sections of TBCs			
100 µm	100 µm	100 µm	100 µm
d) Results of the roughness analysis of the TBCs surfaces			
Ra = 1.7 µm Rsk = 0.41	Ra = 4.2 µm Rsk = 0.35	Ra = 2.8 µm Rsk = - 0.20	Ra = 6.2 µm Rsk = - 0.24

Fig. 3. Analysis of the surface and the cross-section of sol-gel TBCs versus the YSZ fibers percentage in the range 0% and 60% after heat treatment at 1100 °C: (a) photographs of TBCs samples; (b) SEM-FEG micrographs of the surfaces of TBCs; (c) SEM-FEG micrographs of the cross-sections of TBCs; (d) Results of the roughness analysis of the TBCs surfaces.

The coating microstructure was characterized by Scanning Electron Microscope (SEM FEG) JSM 7800F Prime EDS Field Emission Gun (FEG). Surface and sections of TBCs are observed after platinum metallization. Note, for cross sections' micrographs, TBCs are coated in epoxy resin to help cutting. From SEM FEG micrographs of TBC, image analysis was performed with the ImageJ software (GitHub) to determine the porosity percentage into TBC.

The optical microscope 3D Keyence VHX 1000 was used to observe the surface of TBCs and to follow its spalling. The roughness was characterized by a confocal interferometric Zygo New View 100 microscope.

3. Results

3.1. Morphology of TBCs

Samples with a percentage of fibers between 0 %F and 60 %F and sintered at 1100 °C were fabricated by sol gel route (Fig. 3a d). The objective was to determine in which range the TBC will have an optimized lifetime. The appearance of the surface of the TBC gave a first indication of the behavior of the TBC.

According to the macroscopic analysis of the surface of the coating, TBCs are cracked for fiber content lower than 37.5 %F. The cracks initiated at the interface between the TGO and the ceramic coating, and propagated over the entire coating, which is a sign of a brittle coating. On the contrary, when the fiber content was sufficient to form a connected network throughout the material, cracking was only visible in the upper part of the coating (sample at 37.5 %F) or was no longer visible (sample at 60 %F).

Whereas surface roughness is mainly related to cracking for fiber content below 37.5 %F, cracking did not developed for higher fiber content and the increase in roughness was then only related to the presence of fibers at the surface of the sample.

Indeed, for a fiber content of less than 37.5 %F, the roughness (Ra: profile arithmetic average roughness) of the coating was large because of the partial delamination of the TBCs as shown by the positive value of the Rsk parameter (profile asymmetry). Note that without fiber, the coating had a lot of cracks leading to partial delamination of the coating over its entire surface; whereas for a coating with 10% of fibers, cracking was less severe as shown by surface analysis. Between 10% and 37.5% of fibers, the roughness of the coating drops sharply, there is no cracking in the barrier. Whereas the Rsk value for the 10% fibers TBC is positive due to delamination, negative value of Rsk are obtained for the 37.5% of fibers. The observation of the cross sectional coating confirmed this hypothesis: no delamination was observed and porosity is present in the coating leading to a negative value of Rsk. Finally, beyond 37.5 %F, the roughness increased and the Rsk value is negative. This is explained by the increase in the content of fibers in the TBCs, which modifies the surface state and increases the porosity of the coating.

By increasing the content of fibers in the TBCs, cracking is limited and the porosity increases. All these observations tend to confirm that in order to optimize the thermomechanical properties and thus the cyclic oxidation lifetime of the fibrous systems, it is necessary to have fiber content greater than or equal to 37.5 %F.

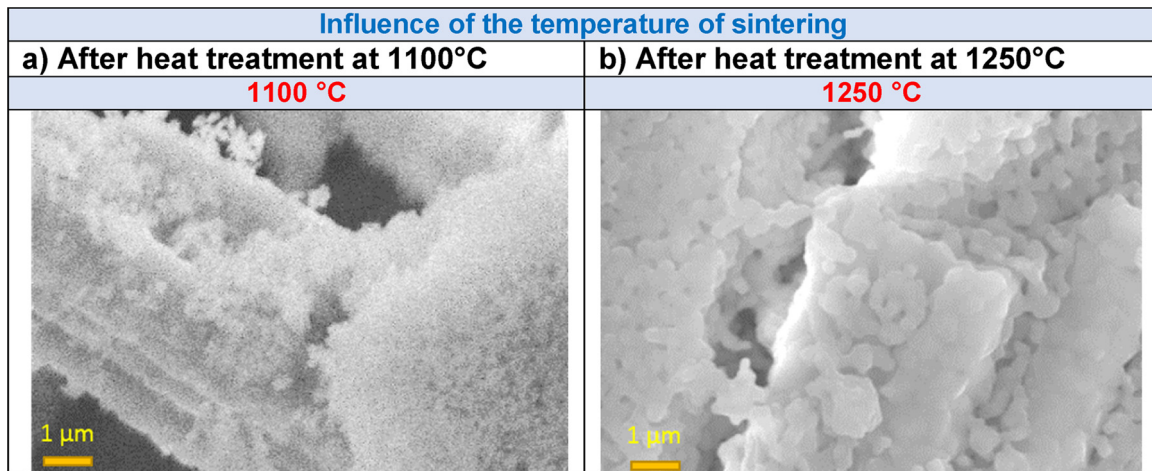Then, the influence of the temperature of thermal treatment was

Influence of the temperature of sintering	
a) After heat treatment at 1100°C	b) After heat treatment at 1250°C
1100 °C	1250 °C

Fig. 4. Influence of the temperature sintering of TBCs: SEM-FEG micrographs: (a) after heat treatment at 1100 °C; (b) after heat treatment at 1250 °C.

studied. TBC sintered at 1250 °C were synthesized. The trends observed for TBCs heat treated at 1250 °C were similar to the ones described above for TBC systems heat treated at 1100 °C. Besides, it seems that the sintering between fibers and powder matrix was improved when TBC were heat treated at 1250 °C (Fig. 4a and b).

Therefore, many TBC were fabricated with a percentage of fibers between 37.5% and 80% and with a sintering at 1250 °C (Fig. 5a e).

The porosity of each sample was measured and it was shown that the porosity increased with the fiber content.

3.2. Behavior of TBCs during cyclic oxidation

A first batch of sol gel thermal barriers with fibers was tested under by cyclic oxidation. Many compositions were studied including TBCs with 37.5%, 50% and 60% of fibers sintered at 1100 °C or at 1250 °C. Two TBCs with 70% and 80% of fibers sintered at 1250 °C were also thermally cycled. The percentages of mass loss and surface spalling are determined for each coating. Fig. 6 shows a summary of results at 20 % S of surface spalling and at 1000 cycles.

3.2.1. Influence of the heat treatment

Two sintering temperatures were tested, 1100 °C and 1250 °C. The temperature of 1100 °C is a standard temperature used to sinter and densify YSZ ceramics and the temperature of 1250 °C is the maximum temperature that the AM1 superalloys can withstand without under going irreversible phase transformations and therefore without being degraded at high temperature.

Sintering at 1250 °C (Fig. 4b) rather than at 1100 °C (Fig. 4a) im proves the cohesion between the fibers and the powder matrix. Bridges are formed between the fibers and the particles with spherical mor phology.

During the cyclic oxidation, the samples were brought to tempera ture at 1100 °C for 1 h. As this temperature is lower than the sintering temperature, the thermochemical stability of the system is guaranteed. Thanks to this thermochemical stability and the improved cohesion of the system, the sol gel thermal barriers sintered at 1250 °C have a better lifetime than those sintered at 1100 °C.

Indeed, for a 20 %S of surface spalling (Fig. 6a), a thermal barrier with 37.5% of fibers has a lifetime of around 200 cycles when sintered at 1100 °C, whereas lifetime is about 450 cycles when the TBC is sin tered at 1250 °C. For a TBCs with 50% of fibers and sintered at 1100 °C, the lifetime is approximately equal to 350 cycles, while it is approxi mately equal to 700 cycles when sintered at 1250 °C. Finally, for a thermal barrier with 60 %F and sintered at 1100 °C, the lifetime is approximately 500 cycles. TBCs sintered at 1250 °C and with a content of fibers between 60 %F and 80 %F have a lifetime superior to 1000

cycles at 20%S of surface spalling. It should be noted that in the last cases, the thermal barrier coatings have a longer life than that of the thermal barrier manufactured by EBPVD.

These results revealed that the influence of the sintering tempera ture on the mechanical properties of porous thermal barriers is im portant, as shown by several studies [9,17,25,28,29]. At 1250 °C, the sintering is improved (Fig. 4b) between fibers and powder matrix. There is a better cohesion in the system between fibers and spherical powder, resulting in a higher fracture toughness.

3.2.2. Influence of the percentage of fibers

From the analysis of the number of cycles reached at 20 %S of surface spalling (Fig. 6a), it is also possible to conclude on the influence of the fiber content on the lifetime of the thermal barrier. Indeed, it is very clear from the results that the lifetime increases with the percen tage of fibers. Furthermore, with the analysis of the surface spalling percentage at 1000 cycles (Fig. 6b), it is also possible to conclude on the optimized range of fiber content to make a sol gel TBCs. Several sam ples were tested to ensure the reproducibility of the TBC behavior and so the repeatability of the sol gel process. Thus, at 1000 cycles, a TBC with 50 %F is completely delaminated (5 samples); while at 60 %F, an average of 15% of surface spalling is observed (10 samples); at 70 %F, the surface spalling is equal to around 6% (6 samples); finally at 80 %F, TBC undergoes around 3% of surface spalling (6 samples).

Thus, the lifetime of a system is optimized for high fiber content. Due to the addition of fibers, the porosity is increased (Fig. 5a e) and this porosity may play a role on the accommodation of the stresses [15]. Moreover, the fibers play a reinforcing role in the composite and im prove the mechanical properties of the ceramic [21]. By increasing the level of fibers into the TBC, mechanical properties are improved and therefore also the lifetime.

From these first tests, it follows that the thermal barriers must be synthesized with high percentage of fibers greater than or equal to 60% of fibers and then sintered at 1250 °C.

3.3. Optimized sol gel TBCs

Sol gel TBC were then fabricated with a percentage of fibers equal to 60 %F, 70 %F and 80 %F and annealed at 1250 °C (Fig. 7a and b).

Porosity increased when increasing the fiber content. About 10 samples with these compositions were manufactured to check the re producibility of the behavior of sol gel TBCs and so the repeatability of the process. Fig. 7 shows a summary of overall results of the surface spalling and the mass loss. For the mass loss, during the first 200 cycles approximately, the mass loss can be attributed to edge effect, so the curves of each TBC are represented without this loss.
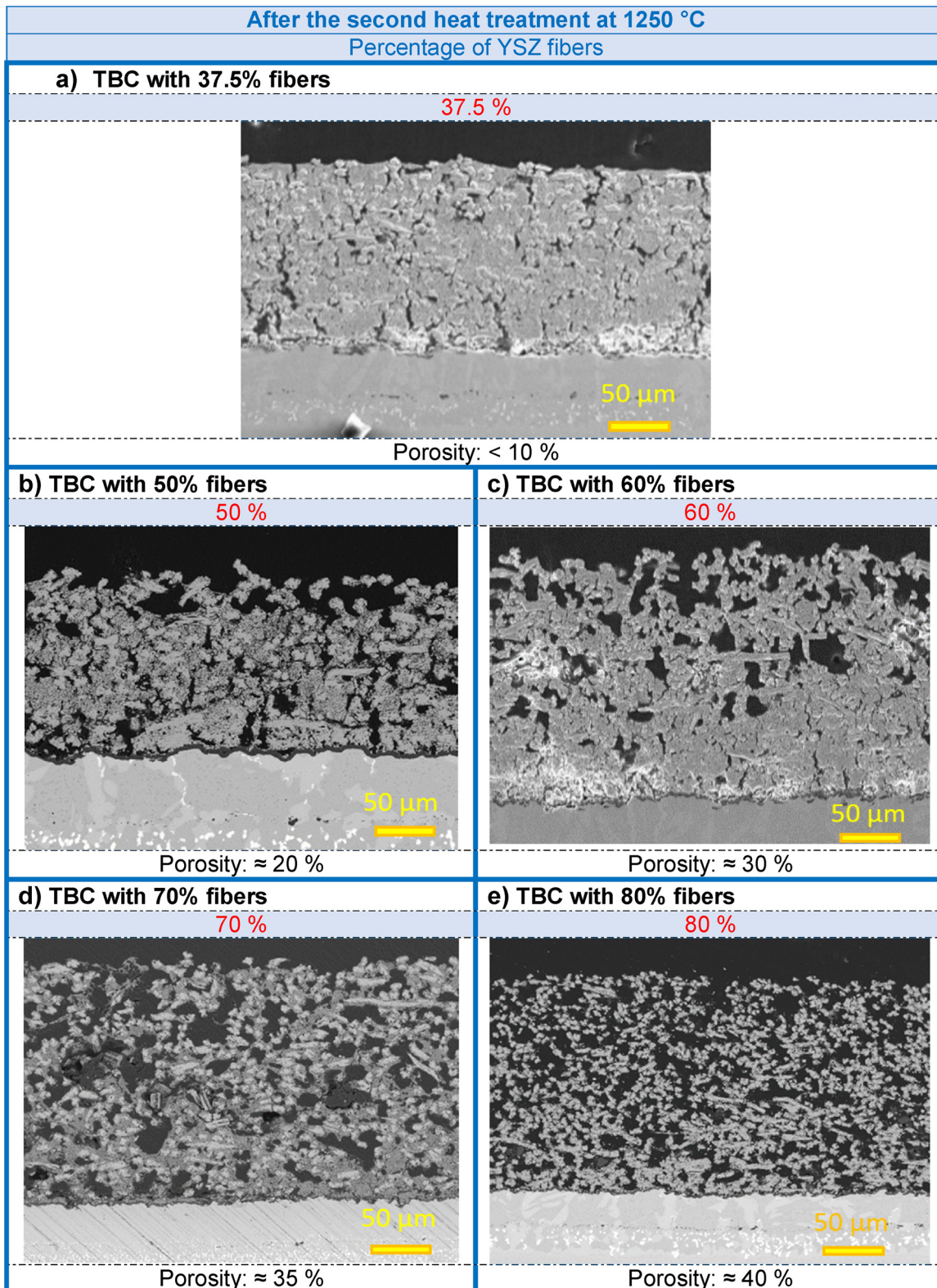
Fig. 5. Cross-sections of TBCs after heat treatment at 1250 °C for different percentages of fibers (SEM-FEG): **(a)** TBC with 37.5% of fibers; **(b)** TBC with 50% of fibers; **(c)** TBC with 60% of fibers; **(d)** TBC with 70% of fibers; **(e)** TBC with 80% of fibers. By image analysis, porosities have been estimated from these micrographs as indicated by values given under the cross-sections.

From the observation of the percentages of mass loss and surface spalling respectively, it can be concluded that *(i)* the lifetime is around 900 cycles for **60% of fibers** (for 21 %m and less than 10 %S); *(ii)* for a system with **70% of fibers**, the lifetimes are higher than to 1000 cycles (for around 16 %m and less than 5 %S); finally, TBC with **80% of fibers** reach 1238 cycles with 19 %m spalling and less than 10 %S. Moreover, for a sample composed of a TBC with 80 %F, the lifetime is greater than 1400 cycles but this result must be checked. Note that TBCs realized by
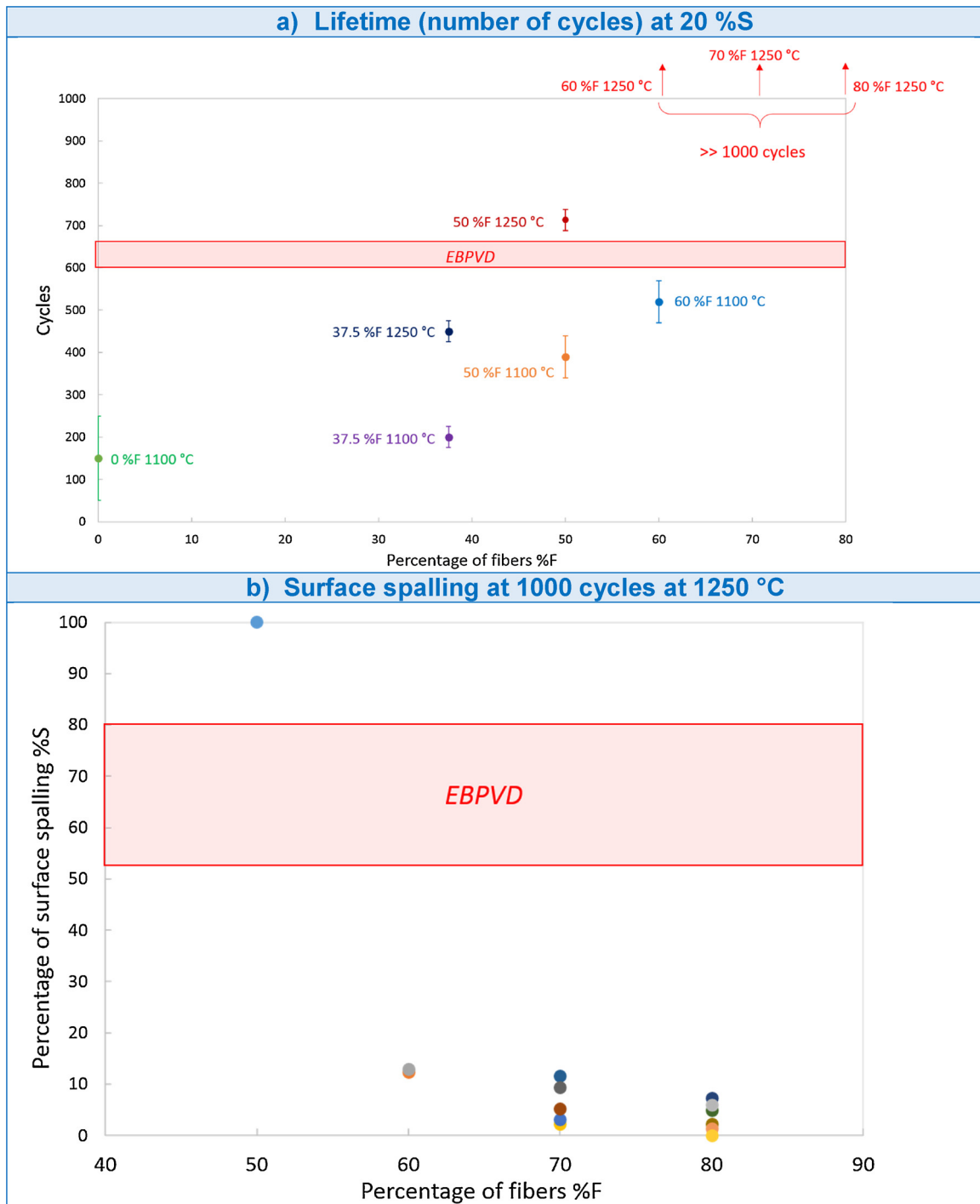
Fig. 6. Comparison between sol-gel TBCs with different fiber contents between 0% and 80%; and sintered at different temperatures: 1100 °C and 1250 °C (between 5 and 8 samples for each composition): (a) number of cycles reached at 20% of surface spalling versus the fiber percentage, (b) percentage of surface spalling versus the fiber percentage for TBCs sintered at 1250 °C.

EBPVD have a lifetime equal to around 600 cycles for 25 %m of mass loss and 20 %S of surface spalling. As expected, the value of the percentages of mass loss is different from the value of the percentage of surface spalling because of the phenomena described above. For each composition, the obtained results appear to be reproducible under cyclic oxidation confirming the reproducibility of the sol gel TBC behavior and therefore the repeatability of sol gel process. TBCs with a percentage of fibers between 60 %F and 80 %F have a better lifetime than TBCs fabricated by EBPVD.

Thus, depending on the industrial standards, several systems based

on fibers can be chosen. If a lifetime of less than 1000 cycles is sufficient, it is possible to choose the system based on 60% of fibers because it is very easy to form in contrast to the system with 80% of fibers which is more delicate to process by dip coating (other technique may be more convenient : spray coating for example). The fibers sediment into the slurry and it is necessary to well stir the slurry between each immersion by dip coating. Nevertheless, with thermal barrier composed of 80 %F, the lifetime of the ceramic is greater than 1200 cycles. In order to have both the ease of shaping and a lifetime of more than 1100 cycles, the intermediate choice is to develop a ceramic coating based on 70% of
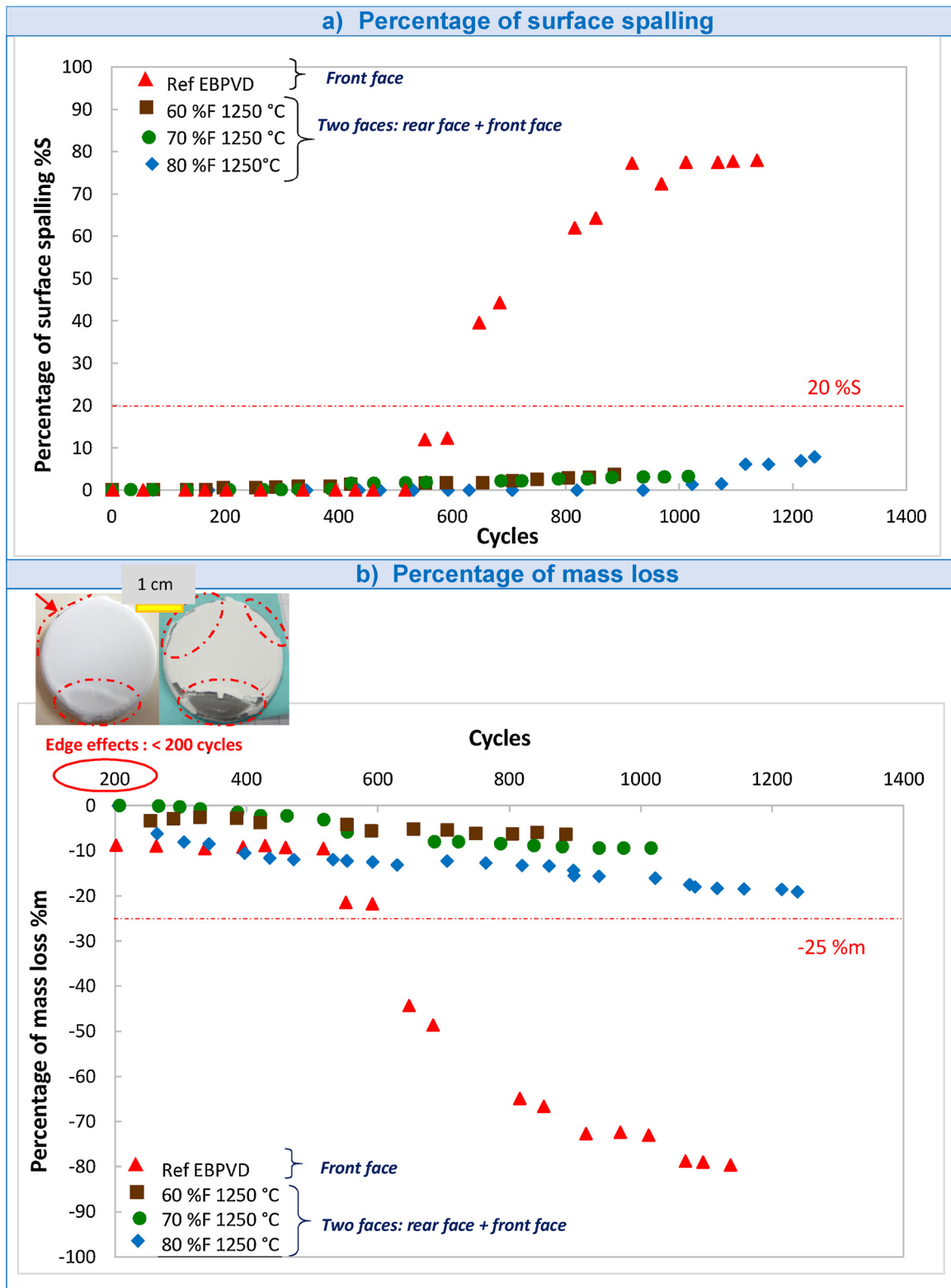
Fig. 7. Overall results of cyclic oxidation of the best sol-gel TBCs: (a) percentage of surface spalling versus the number of cycles, (b) mass loss versus the number of cycles (visualization of edge effects caused by sol-gel process and dip-coating technique).

fibers.

As a remark, it has been proved that sol gel thermal barriers fabricated from aerogel are subjected to delamination in the form of islands [11,30] whereas the delamination of thermal barriers made by EBPVD occurs by the loss of large ceramics pieces [5,31,32]. Thus, the degradation mode of fiber based thermal barriers approaches the

degradation mode of EBPVD systems with delamination of large spalls of coating.

Note that YSZ ceramic of TBCs keeps its metastable tetragonal phase t', a Raman spectroscopy analysis confirms this result (Fig. 8). Indeed, during all steps of the process; i.e. after elaboration by dip coating, after heat treatment of sintering at 1250 °C and before cyclic oxidation, and,
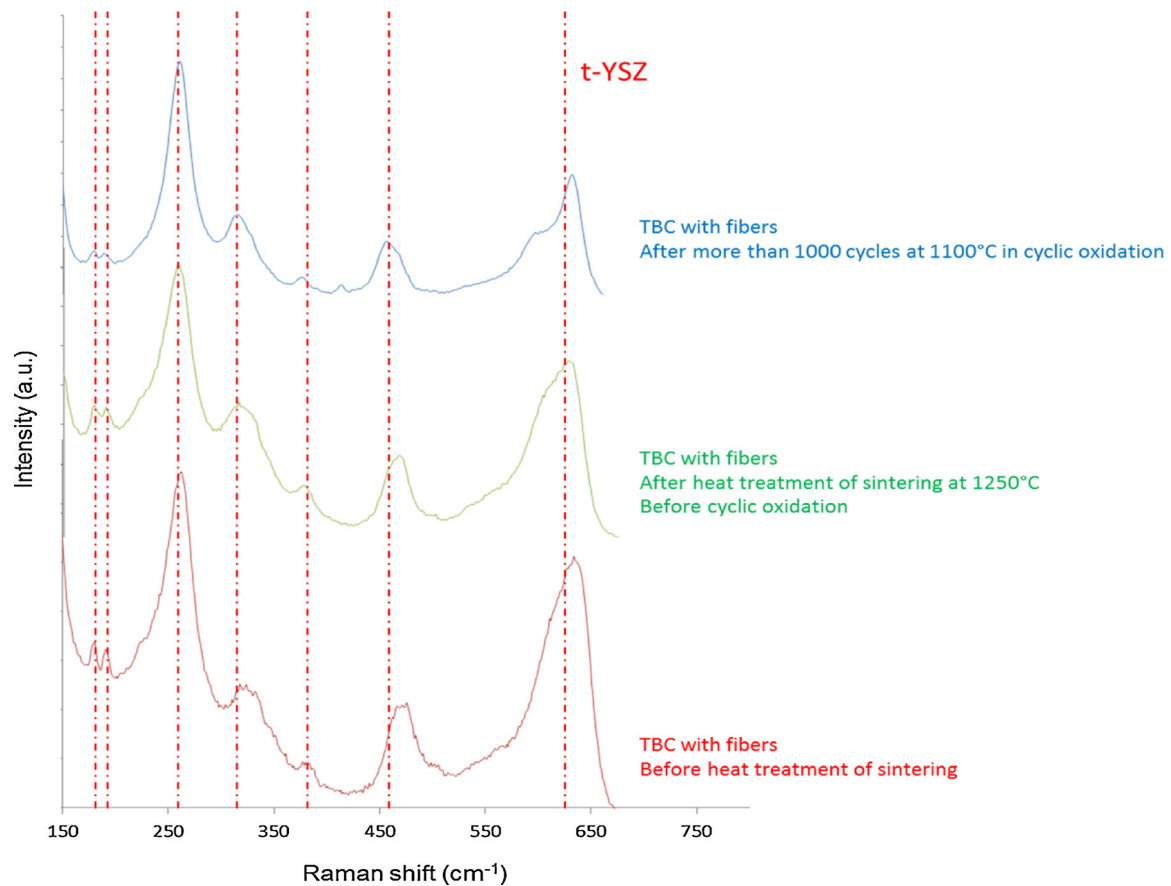
Fig. 8. Raman spectroscopies of YSZ ceramic of TBCs: *(i)* before heat treatment of sintering, *(ii)* after heat treatment of sintering at 1250 °C and before cyclic oxidation, finally *(iii)* after more than 1000 cycles at 1100 °C in cyclic oxidation.

finally, after more than 1000 cycles at 1100 °C in cyclic oxidation; there is no phase transformation into monoclinic phase.

4. Discussion

4.1. Effect of TBC porosity

With increasing the content of fibers, the percentage of porosity increases (Fig. 5a e). Currently, TBC manufactured by APS or EBPVD have a porosity of about 15% According to the present study, sol gel TBCs composed of 60 80% of fibers, have an optimized lifetime under cyclic oxidation. However, their percentage of porosity is between 30% and 40%. So, the porosity of these systems is greater than that of in dustrial systems. Moreover, with the sol gel process, the morphology of TBC is uniform and equiaxed. Then, fibers are uniformly dispersed in the coatings. TBCs fabricated by EBPVD exhibits a porous columnar microstructure resulting a quite high strain tolerance; and TBC realized by APS has a lamellar dense microstructure resulting a weaker strain tolerance. It appears that the fibers in the sol gel TBC allow obtaining a resistance to thermal cycling better than EBPVD TBCs, despite an equiaxed microstructure and a higher porosity. A higher porosity may have also a positive effect on the thermal conductivity. Nevertheless, the higher porosity may be detrimental to erosion resistance and this will have to be tested in the future.

4.2. Improvement of mechanical properties thanks to crack deviation in TBCs

During this study, the cracking was studied and it appeared that the fibers make it possible to limit the cracking by deviating or blocking it.

It was observed by microscopy that the cracks are deflected or blocked by YSZ fibers (Fig. 9a c).

Moreover, this phenomenon was present for each fiber content and the temperature of the sintering. In addition to generating porosity thanks to their internal porosity and their entanglement within the powder matrix, the fibers succeed in deflecting and limiting the cracking. Indeed, various studies [33 40], in civil engineering for ex ample, attest to the beneficial effect of fibers on limiting crack bridging. Abdi et al. [36] have proved that the clay reinforcement by the fibers makes it possible to reduce the cracking and to limit it. Nair [35] has also demonstrated their interest in bridging cracks, reducing cracking and improving the mechanical properties of composites. Several studies have already shown the advantages of adding fibers in ceramics in order to improve thermomechanical properties [20 24]. It would ap pear that in the case of sol gel thermal barriers, the fibers also make it possible to optimize the thermomechanical properties.

In order to better understand the degradation mode of thermal barriers composed of fibers, the TGO layer must be analyzed because delamination of the thermal barrier depends mainly on the degradation mode of the TGO layer.

4.3. Improvement of mechanical properties thanks to TGO

The degradation of the thermal barrier during high temperature cyclic oxidation depends on the thermomechanical behavior of the TGO alumina layer [3,5,41].

TGO layer is characterized: *(i)* after pre oxidation of the β (Ni, Pt)Al coated AM1 superalloy at 1100 °C for 1 h, *(ii)* after the sintering heat treatment at 1250 °C for 2 h made on the complete TBC system and *(iii)* after 800 cycles at 1100 °C. Many samples were analyzed to check the
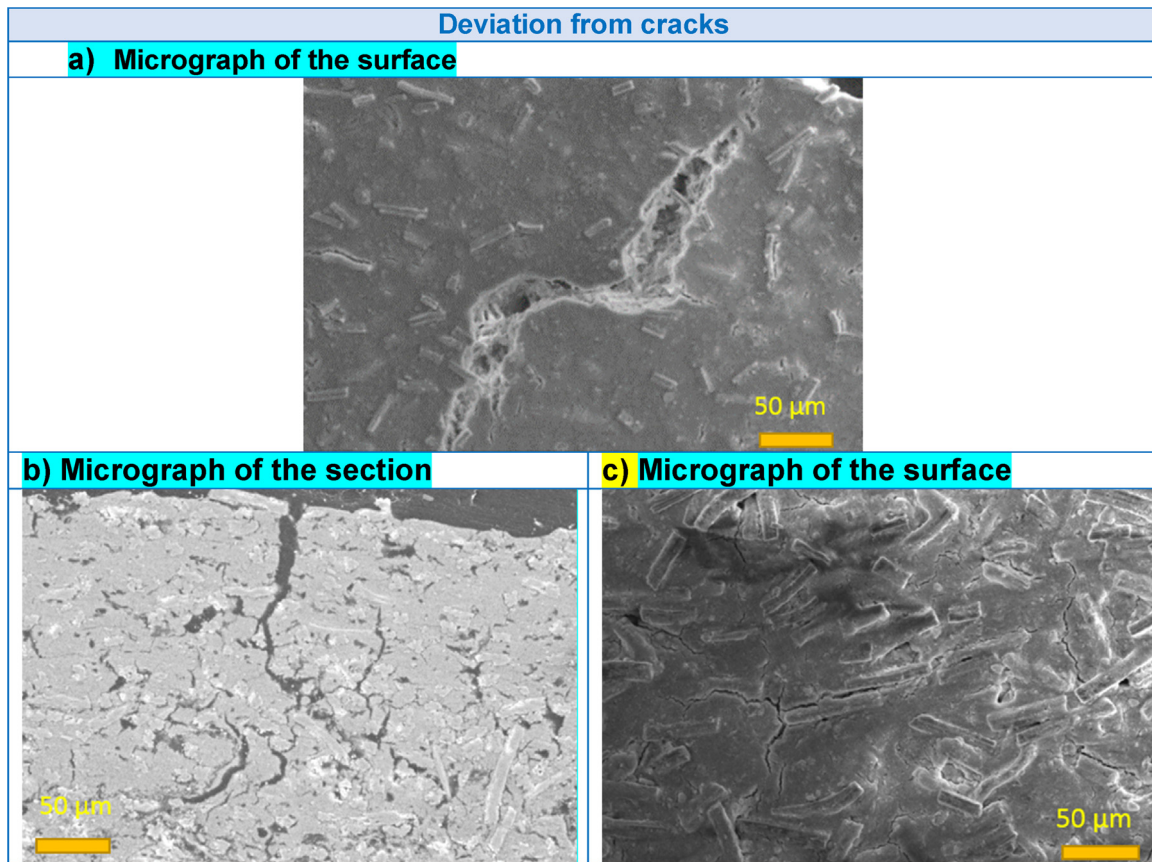
Fig. 9. SEM-FEG analysis of TBCs with 37.5% of fibers and sintered at 1250 °C: (a) micrograph of the surface; (b) micrograph of the section; (c) micrograph of the surface.

reproducibility of the results (about ten samples in each case). According to the fluorescence spectroscopy Raman analysis, the TGO layer is composed only of α alumina (no transient alumina is detected) (Fig. 10a). Thanks to this phase, the TBCs are not impacted by phase transformation during cyclic oxidation. Based on SEM micrographs (Fig. 10b), the TGO thickness after pre oxidation is equal to about 1 μm, as already mentioned. After the heat treatment carried out to sinter the ceramic coating, its thickness is equal to about 3 μm. Finally after more than 800 cycles at 1100 °C, its thickness is equal to about 8 μm. To compare with results, for an EBPVD system on the same substrate, the TGO thickness will increase from 0.4 μm after manufacturing and 6 8 μm after 500 700 cycles (duration: 1 h) at 1100 °C. So, this differ ence in initial thickness before cyclic oxidation has to be taken into account when comparing these two types of systems. Indeed, with a higher layer thickness, the sol gel TBC composed of fibers has a longer lifetime than EBPVD TBC in cyclic oxidation, which shows the interest of the fibers.

The TGO layer grows during the cyclic oxidation, resulting in stress. In addition, the difference in coefficient of thermal expansion between the materials (thermal barrier, TGO, bond coat and superalloy) leads to compressive stresses within the TGO, during cooling. When these stresses become too important, cracking occurs. Cracking can propagate at the bond coat/TGO interface (adhesive rupture), within the TGO (cohesive rupture) and/or at the TGO/TBC interface (adhesive rupture), leading the loss of the thermal barrier by spalling.

Thermal barriers fabricated from fibers do not have exactly the same degradation model as those of the thermal barriers made by EBPVD or by sol gel via the aerogel powder. Indeed, the EBPVD thermal barriers undergo delamination because of the buckling of the ceramic coating, there is a weaker adhesion between the latter and the metal substrate, and because of the high coefficients of expansion of these two

systems, the TGO layer undergoes thermomechanical stresses leading to the delamination of the thermal barrier at its interface. On the other hand, for thermal barriers made from aerogel powder via the sol gel process, the ceramic coating delaminates in the form of islands, because there is a relatively large adhesion between the thermal barrier and the TGO. Due to the high stresses within the TGO, the ceramic coating undergoes crack by shearing, which results in spalling of ceramics is lets. Fiber based thermal barriers are an intermediate system. Indeed, during the growth of the TGO, the sintering heat treatment and the cyclic oxidation, the TGO could find points of anchorage in the fibers (Fig. 11a) and thus grow around the ceramic thus ensuring a better cohesion of the system (Fig. 11b) and higher toughness. This could explain the phenomena of adhesive failure at the interface between the TGO layer and the bond coat, and the cohesive rupture within the TGO layer (Fig. 11b).

5. Conclusions

Innovative thermal barrier coatings were fabricated by a sol gel route using commercial powder. YSZ fibers and powders with a sphe rical morphology were used. The effects of the percentage of fibers and the sintering temperature of the thermal barriers were studied. To ob tain an optimized performance, it was necessary to fabricate a thermal barrier coating with a percentage of fibers between 60% and 80% and a temperature of thermal treatment equal to 1250 °C.

Under cyclic oxidation, these systems exhibited a longer lifetime as compared to a system composed of an EBPVD thermal barrier. The lifetime, greater than 1000 1 h cycles at 1100 °C for 20% of surface spalling and 25 %m of mass loss, was improved by increasing the fiber content. Moreover, for a fiber content of 80 %, a sol gel TBC system reached a lifetime greater than 1400 cycles; while the EBPVD TBC had a
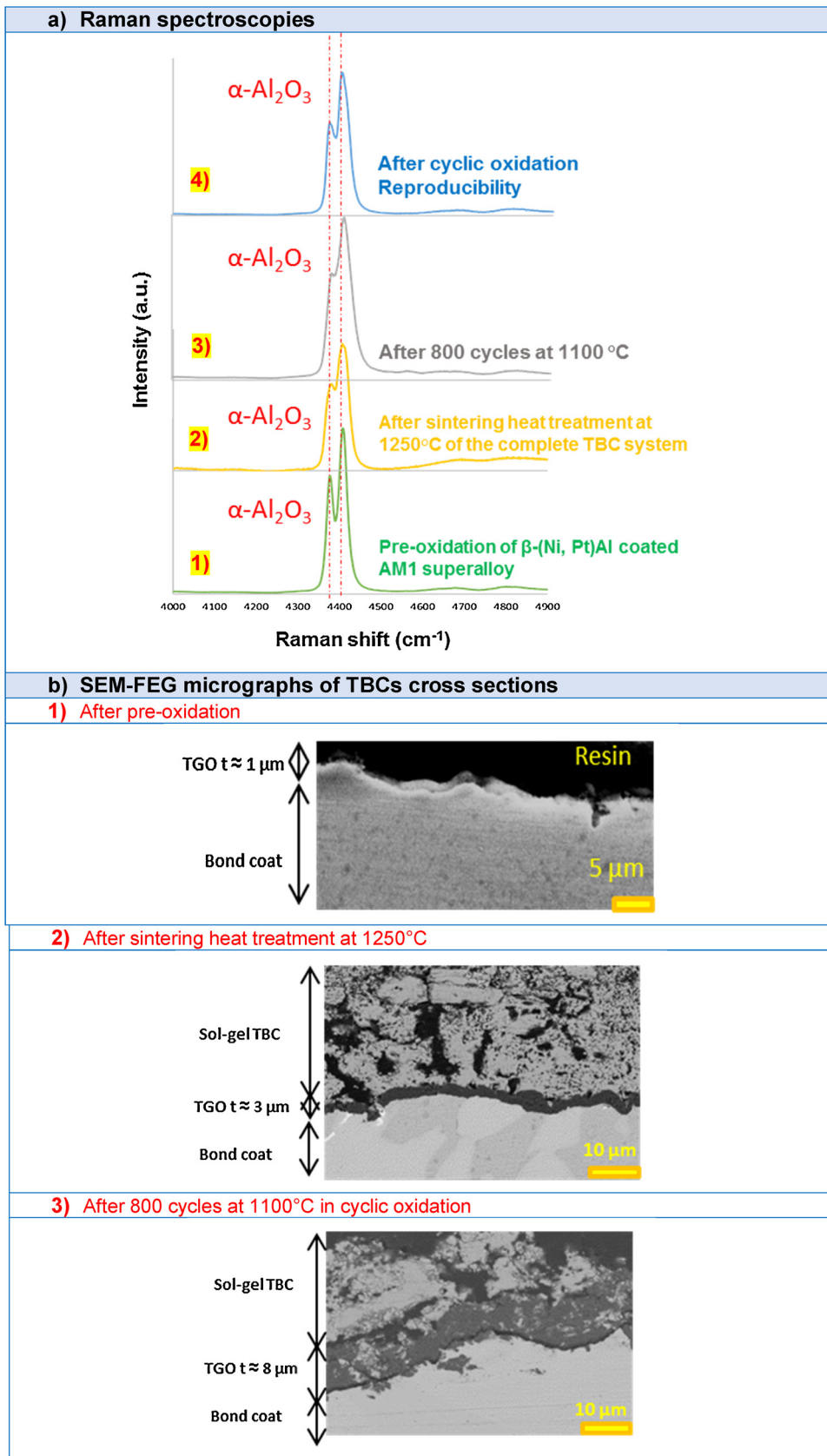
Fig. 10. Analysis of α-Al₂O₃ phase of TGO: **(a)** Raman spectroscopies of the TGO after: *(1)* pre-oxidation, *(2)* sintering heat treatment at 1250 °C; *(3)* 800 cycles at 1100 °C; *(4)* reproducibility check after cyclic oxidation (more than 1000 cycles) ; **(b)** SEM-FEG micrographs of TBCs cross sections observed after: *(1)* pre-oxidation, *(2)* sintering heat treatment at 1250 °C; *(3)* 800 cycles at 1100 °C.
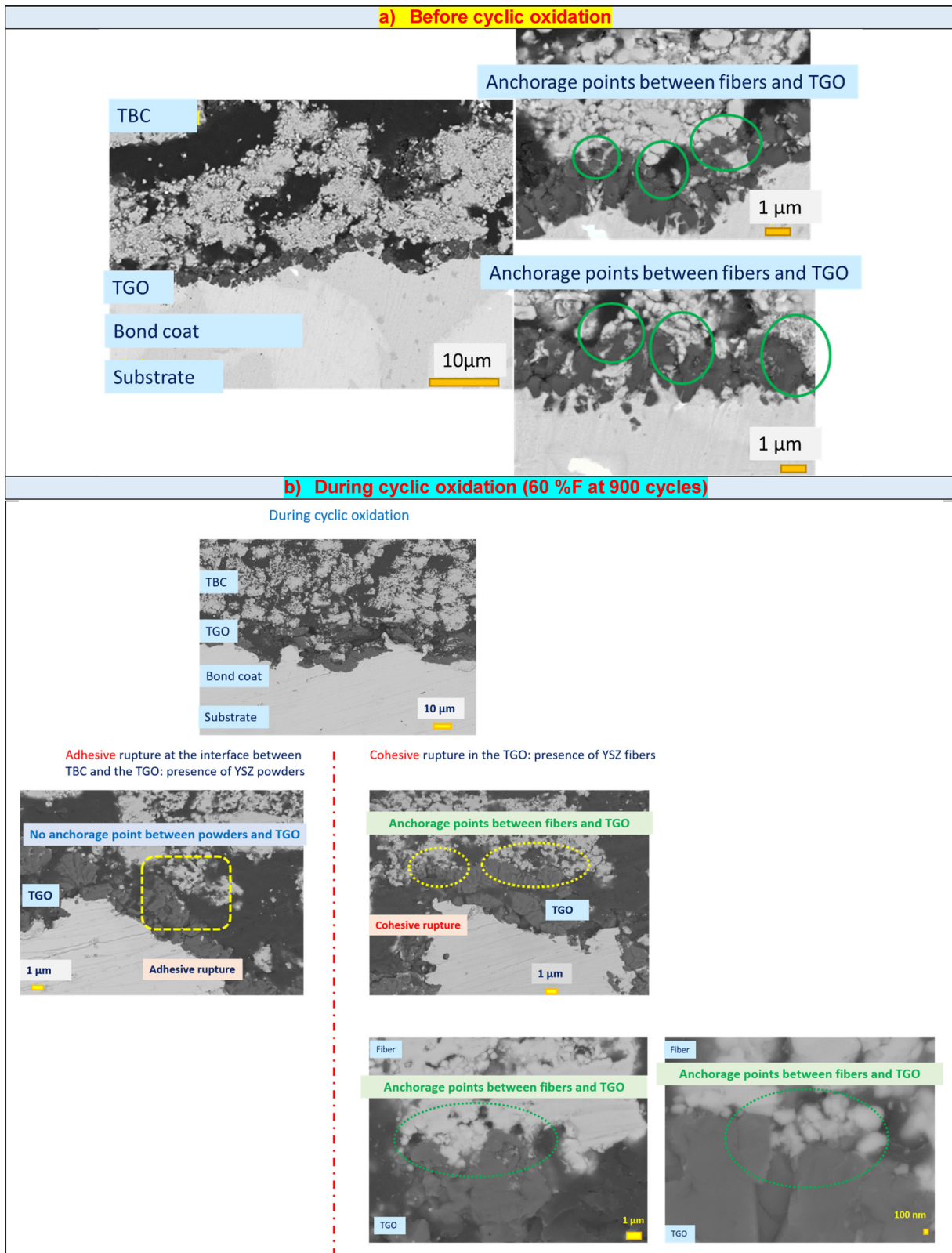
Fig. 11. SEM-FEG micrographs of the sections of TBCs to observe anchorage points between fibers and TGO layer: (a) before cyclic oxidation; (b) during cyclic oxidation (TBC with 60 %F at 900 cycles).

lifetime equal to about 600 cycles in the same condition and with the same substrate. Moreover, the reproducibility of these thermal barriers and so the repeatability of the sol gel process have been verified for about ten samples. Finally, the degradation mode of sol gel TBCs composed of fibers is intermediate to the one of EBPVD TBCs and the one of sol gel TBCs based on an aerogel powder. Indeed fibers make points of anchorage with the TGO layer improving the cohesion of the system.

Mechanical properties of TBCs are improved thanks to fibers. Indeed, fibers allow deflecting the cracks and reducing the cracking. Furthermore, thanks to the sol gel process, fibrous ceramics are homogeneously dispersed and highly adherent to the powder matrix. The morphology of these systems is then uniform and equiaxed. The percentage of porosity increases with the content of fibers into TBC. The consequence of porosity on thermal and erosion properties needs to be studied, as well as porosity effect on mechanical properties for a con stant density of fibers. Fibers serve as anchors for the TGO layer and thanks to this phenomenon, the adherence between the ceramic top coat and the TGO layer is improved as well as the lifetime of the system.

For further study, it would be possible to fabricate the fibrous TBCs by sol gel route on specific shaped substrates intended to be tested under cyclic oxidation to overcome problems related to the edge effects. The TGO could be analyzed at different cycles, for example every 200 cycles, to observe its growth and so the progressive delamination of TBC. Moreover, rather than using YSZ ceramic with a tetragonal me tastable phase t', TBC could be elaborate with a tetragonal metastable phase t''. Then, the self healing technology of TBCs could be added to these systems [9].

To conclude, these thermal barrier coatings made by a sol gel route with fibrous YSZ ceramics are possible competitors to the classical TBC systems. Indeed, this sol gel process has many advantages in terms of process cost, complex shape coating and reparability.

Acknowledgements

References

[1] U. Schulz, C. Leyens, K. Fritscher, M. Peters, B. Saruhan-Brings, O. Lavigne, J.M. Dorvaux, M. Poulain, R. Mevrel, M. Caliez, Some recent trends in research and technology of advanced thermal barrier coatings, Aerosp. Sci. Technol 7 (2003) 73–80.

[2] M. Peters, C. Leyens, U. Schulz, W.A. Kaysser, EB-PVD thermal barrier coatings for aeroengines and gas turbines, Eng. Mater. 3 (4) (2001) 193–204.

[3] A.G. Evans, D.R. Mumm, J.W. Hutchinson, G.H. Meier, F.S. Pettit, Mechanisms controlling the durability of thermal barrier coatings, Prog. Mater. Sci. 46 (5) (2001) 505–553.

[4] T. Tomimatsu, S. Zhu, Y. Kagawa, Effect of thermal exposure on stress distribution in TGO layer of EB-PVD TBC, Acta Mater. 51 (8) (2003) 2397–2405.

[5] P.K. Wright, A.G. Evans, Mechanisms governing the performance of thermal barrier coatings, Curr. Opin. Solid State Mater. Sci. 4 (3) (1999) 255–265.

[6] O. Trunova, T. Beck, R. Herzog, R.W. Steinbrech, L. Singheiser, Damage mechanisms and lifetime behavior of plasma sprayed thermal barrier coating systems for gas turbines—part I: experiments, Surf. Coat. Technol. 202 (20) (2008) 5027–5032.

[7] A. Rabiei, A.G. Evans, Failure mechanisms associated with the thermally grown oxide in plasma-sprayed thermal barrier coatings, Acta Mater. 48 (15) (2000) 3963–3976.

[8] B. Bernard, A. Quet, L. Bianchi, V. Schick, A. Joulia, A. Malié, B. Rémy, Effect of suspension plasma-sprayed YSZ columnar microstructure and bond coat surface preparation on thermal barrier coatings properties, J. Therm. Spray Technol. 26 (6) (2017) 1025–1037.

[9] F. Nozahic, D. Monceau, C. Estournès, Thermal cycling and reactivity of a MoSi$_2$/ZrO$_2$ composite designed for self-healing thermal barrier coatings, Mater. Des. 94 (Macrh) (2016) 444–448.

[10] N.K. Eils, P. Mechnich, W. Braue, Effect of CMAS deposits on MOCVD coatings in the system Y$_2$O$_3$ -ZrO$_2$: phase relationships, J. Am. Ceram. Soc. (August) (2013) n/a-n/a.

[11] L. Pin, et al., Optimized sol–gel thermal barrier coatings for long-term cyclic oxidation life, J. Eur. Ceram. Soc. 34 (4) (2014) 961–974.

[12] M. Bai, F. Guo, P. Xiao, Fabrication of thick YSZ thermal barrier coatings using electrophoretic deposition, Ceram. Int. 40 (10) (2014) 16611–16616.

[13] J. Zhou, C.-A. Wang, Porous yttria-stabilized zirconia ceramics fabricated by non-aqueous-based gelcasting process with PMMA microsphere as pore-forming agent, J. Am. Ceram. Soc. 96 (1) (2013) 266–271.

[14] R. Liu, C. Wang, Effects of mono-dispersed PMMA micro-balls as pore-forming agent on the properties of porous YSZ ceramics, J. Eur. Ceram. Soc. 33 (10) (2013) 1859–1865.

[15] T. Clyne, I. Golosnoy, J. Tan, A. Markaki, Porous materials for thermal management under extreme conditions, Philos. Trans. R. Soc. Math. Phys. Eng. Sci. 364 (January (1838)) (2006) 125–146.

[16] K.W. Schlichting, N.P. Padture, P.G. Klemens, Thermal conductivity of dense and porous yttria-stabilized zirconia, J. Mater. Sci. 36 (12) (2001) 3003–3010.

[17] L. Hu, C.-A. Wang, Y. Huang, Porous yttria-stabilized zirconia ceramics with ultra-low thermal conductivity, J. Mater. Sci. 45 (12) (2010) 3242–3246.

[18] L. Pin, F. Ansart, J.-P. Bonino, Y. Le Maoult, V. Vidal, P. Lours, Processing, repairing and cyclic oxidation behaviour of sol–gel thermal barrier coatings, Surf. Coat. Technol. 206 (7) (2011) 1609–1614.

[19] L. Pin, F. Ansart, J.-P. Bonino, Y. Le Maoult, V. Vidal, P. Lours, Reinforced sol–gel thermal barrier coatings and their cyclic oxidation life, J. Eur. Ceram. Soc. 33 (2) (2013) 269–276.

[20] Y. Lang, Y. Dong, J. Zhou, C.-A. Wang, YSZ fiber-reinforced porous YSZ ceramics with lowered thermal conductivity: influence of the sintering temperature, Mater. Sci. Eng. A 600 (2014) 76–81.

[21] Y. Dong, C.-A. Wang, J. Zhou, Z. Hong, A novel way to fabricate highly porous fibrous YSZ ceramics with improved thermal and mechanical properties, J. Eur. Ceram. Soc. 32 (10) (2012) 2213–2218.

[22] Y. Lang, C.-A. Wang, Al2O3-fiber-reinforced porous YSZ ceramics with high mechanical strength, Ceram. Int. 40 (August (7)) (2014) 10329–10335.

[23] J. Sun, Z. Hu, J. Li, H. Zhang, C. Sun, Thermal and mechanical properties of fibrous zirconia ceramics with ultra-high porosity, Ceram. Int. 40 (8) (2014) 11787–11793.

[24] R. Zhang, X. Hou, C. Ye, B. Wang, Enhanced mechanical and thermal properties of anisotropic fibrous porous mullite–zirconia composites produced using sol-gel impregnation, J. Alloys Compd. 699 (2017) 511–516.

[25] M. Yashima, M. Kakihana, M. Yoshimura, Metastable-stable phase diagrams in the zirconia-containing systems utilized in solid-oxide fuel cell application, Solid State Ionics 86-88 (1996) 1131–1149.

[26] C.H. Perry, D.-W. LIU, R.P. INGEL, Phase characterization of partially stabilized zirconia by Raman spectroscopy, J. Am. Ceram. Soc. 68 (8) (1985).

[27] M. Yashima, K. Ohtake, Determination of cubic-tetragonal phase boundary in Zr1-xYxO2-x/2 solid solutions by Raman spectroscopy, J. Appl. Phys. 74 (12) (1993) 7603–7605.

[28] L. Hu, C.-A. Wang, Effect of sintering temperature on compressive strength of porous yttria-stabilized zirconia ceramics, Ceram. Int. 36 (5) (2010) 1697–1701.

[29] G.-J. Yang, Z.-L. Chen, C.-X. Li, C.-J. Li, Microstructural and mechanical property evolutions of plasma-sprayed YSZ coating during high-temperature exposure: comparison study between 8YSZ and 20YSZ, J. Therm. Spray. Technol. 22 (8) (2013) 1294–1302.

[30] J. Sniezewski, et al., Sol–gel thermal barrier coatings: optimization of the manufacturing route and durability under cyclic oxidation, Surf. Coat. Technol. 205 (5) (2010) 1256–1261.

[31] A. Strawbridge, H.E. Evans, Mechanical failure of thin brittle coatings, Eng. Fail. Anal. 2 (2) (1995) 85–103.

[32] P. Bansal, P.H. Shipway, S.B. Leen, Finite element modelling of the fracture behaviour of brittle coatings, Surf. Coat. Technol. 200 (18–19) (2006) 5318–5327.

[33] J.W.C. Pang, I.P. Bond, A hollow fibre reinforced polymer composite encompassing self-healing and enhanced damage visibility, Compos. Sci. Technol. 65 (11–12) (2005) 1791–1799.

[34] H. Stang, V.C. Li, Classification of fiber reinforced cementitious materials for structural applications, Proc. BEFIB (2004) 197–218.

[35] S.V. Nair, Crack-wake debonding and toughness in fiber-or whisker-reinforced brittle-matrix composites, J. Am. Ceram. Soc. 73 (10) (1990) 2839–2847.

[36] M.R. Abdi, A. Parsapajouh, M.A. Arjomand, Effects of random fiber inclusion on consolidation, hydraulic conductivity, swelling, shrinkage limit and desiccation cracking of clays, Int. J. Civ. Eng. 6 (4) (2008) 284–292.

[37] P.S. Song, S. Hwang, B.C. Sheu, Strength properties of nylon- and polypropylene-fiber-reinforced concretes, Cem. Concr. Res. 35 (8) (2005) 1546–1550.

[38] S.A. Hayes, F.R. Jones, K. Marshiya, W. Zhang, A self-healing thermosetting composite material, Compos. Part Appl. Sci. Manuf. 38 (4) (2007) 1116–1120.

[39] G. Williams, R. Trask, I. Bond, A self-healing carbon fibre reinforced polymer for aerospace applications, Compos. Part Appl. Sci. Manuf. 38 (6) (2007) 1525–1532.

[40] T. Matsumoto, V.C. Li, Fatigue life analysis of fiber reinforced concrete with a fracture mechanics based model, Cement Concrete Comp. 21 (1999) 249–261.

[41] H.E. Evans, Oxidation failure of TBC systems: an assessment of mechanisms, Surf. Coat. Technol. 206 (7) (2011) 1512–1521.